Research

The Response of the Root Proteome to the Synthetic Strigolactone GR24 in *Arabidopsis*

Alan Walton‡§¶‖[c], Elisabeth Stes‡§¶‖[c], Geert Goeminne‡§, Lukas Braem‡§, Marnik Vuylsteke, Cedrick Matthys‡§, Carolien De Cuyper‡§, An Staes¶‖, Jonathan Vandenbussche¶‖, François-Didier Boyer‡‡§§¶¶, Ruben Vanholme‡§, Justine Fromentin‡§‖‖[a], Wout Boerjan‡§, Kris Gevaert¶‖[bc], and Sofie Goormachtig‡§[bc]**

Strigolactones are plant metabolites that act as phytohormones and rhizosphere signals. Whereas most research on unraveling the action mechanisms of strigolactones is focused on plant shoots, we investigated proteome adaptation during strigolactone signaling in the roots of *Arabidopsis thaliana.* Through large-scale, time-resolved, and quantitative proteomics, the impact of the strigolactone analog *rac*-GR24 was elucidated on the root proteome of the wild type and the signaling mutant *more axillary growth 2 (max2)*. Our study revealed a clear MAX2-dependent *rac*-GR24 response: an increase in abundance of enzymes involved in flavonol biosynthesis, which was reduced in the *max2–1* mutant. Mass spectrometry-driven metabolite profiling and thin-layer chromatography experiments demonstrated that these changes in protein expression lead to the accumulation of specific flavonols. Moreover, quantitative RT-PCR revealed that the flavonol-related protein expression profile was caused by *rac*-GR24-induced changes in transcript levels of the corresponding genes. This induction of flavonol production was shown to be activated by the two pure enantiomers that together make up *rac*-GR24. Finally, our data provide much needed clues concerning the multiple roles played by MAX2 in the roots and a comprehensive view of the *rac*-GR24-induced response in the root proteome. ***Molecular & Cellular Proteomics 15: 10.1074/mcp.M115.050062, 2744–2755, 2016.***

Root development is pivotal for plant survival, providing anchorage, ensuring water and nutrient uptake, and allowing the plant to engage in beneficial interactions with soil microorganisms. Root growth is modulated in response to numerous abiotic and biotic environmental cues, which are interpreted and transduced by hormonal pathways. Besides the well-known regulators of root development, such as auxin and cytokinin, a group of carotenoid-derived terpenoid lactones, coined strigolactones, have been described to play a role in the regulation of root architecture. The influence of strigolactones on the lateral root density (LRD)[1], adventitious root formation, and induction of root hair elongation has been demonstrated, but the molecular networks ruling these belowground effects are still not well understood (1–7).

Multiple research teams have contributed to a better understanding of the strigolactone biosynthesis pathway, early signaling processes, and transport mechanisms (8–14). Early signaling occurs mainly through the action of an α/β-hydrolase DWARF14 (D14)/DECREASED APICAL DOMINANCE2 (DAD2) that interacts with an F-box protein, MORE AXILLARY GROWTH2 (MAX2) (15). MAX2 together with an additional α/β-hydrolase and a D14 paralog, KARRIKIN INSENSITIVE2

From the ‡Department of Plant Systems Biology, VIB, 9052 Ghent, Belgium; §Department of Plant Biotechnology and Bioinformatics, Ghent University, 9052 Ghent, Belgium; ¶Medical Biotechnology Center, VIB, 9000 Ghent, Belgium; ‖Department of Biochemistry, Ghent University, 9000 Ghent, Belgium; **Gnomixx, 9000 Ghent, Belgium; ‡‡Institut National de la Recherche Agronomique, Institut Jean-Pierre Bourgin, Unité Mixte de Recherche 1318, Equipe de Recherche Labellisée Centre National de la Recherche Scientifique 3559, Saclay Plant Sciences, 78026 Versailles, France; §§AgroParisTech, Institut Jean-Pierre Bourgin, Unité Mixte de Recherche 1318, Equipe de Recherche Labellisée Centre National de la Recherche Scientifique 3559, Saclay Plant Sciences, 78026 Versailles, France; ¶¶Centre de Recherche de Gif, Institut de Chimie des Substances Naturelles, Unité Propre de Recherche 2301, Centre National de la Recherche Scientifique, 91198 Gif-sur-Yvette, France, ‖‖Laboratoire des Interactions Plantes-Microorganismes, Unité Mixte de Recherche 441, Institut National de la Recherche Agronomique, 31326 Castanet-Tolosan, France; and [a]Laboratoire des Interactions Plantes-Microorganismes, Unité Mixte de Recherche 2594, Centre National de la Recherche Scientifique, 31326 Castanet-Tolosan, France

Received March 30, 2015, and in revised form, June 9, 2016
Published, MCP Papers in Press, June 17, 2016, DOI 10.1074/mcp.M115.050062
Author contributions: A.W., E.S., K.G., and S.G. designed research; A.W., E.S., G.G., L.B., M.V., C.M., C.D.C., A.S., J.V., F.-D.B., and J.F. performed research; A.W., E.S., G.G., and R.V. analyzed data; A.W., E.S., K.G., and S.G. wrote the paper.

[1] The abbreviations used are: C4H, cinnamate-4-hydroxylase; CFI, chalcone flavone isomerase; CHS, chalcone synthase; D14, DWARF14; DAD, DECREASED APICAL DOMINANCE; DPBA, diphenylboric acid 2-amino ethyl ester; F3H, flavanone 3-hydroxylase; FLS, flavonol synthase; GO, gene ontology; HPLTC, high-performance thin-layer chromatography; hpt, hours post treatment; HTL, HYPOSENSITIVE TO LIGHT; KAI, KARRIKIN INSENSITIVE; LRD, lateral root density; LTQ, linear trap quadrupole; MAX, MORE AXILLARY GROWTH; MS, Murashige and Skoog; NAP, nonintrinsic ABC protein; PAL, phenyl ammonia-lyase; PIN, PIN-FORMED; *rac*-GR24, strigolactone analog; UGT, UDP-glucosyl transferase; ULPC, ultra-performance liquid chromatography; WT, wild type.

(KAI2), also mediates the response to smoke-derived karrikins (16) as well as to certain strigolactone analogs (17, 18). The capacity of both the D14 and KAI2 proteins to recognize strigolactone analogs has been reported to be stereospecific (18). MAX2 is part of a Skp, Cullin, F-box-containing (SCF^{MAX2}) complex (19, 20), which, in response to the hormone, gives rise to the ubiquitination of specific targets leading to their proteasomal degradation. Various members of the SUPPRESSOR OF MAX2-LIKE (SMXL) family have been identified that have shown to be the targets of this SCF complex (21–25).

Indeed, the initial discovery of the hormonal action of strigolactones was based on a set of high branching or high tillering mutants in various plant species, (19, 26–29). However, an increasing number of studies demonstrate a role for this hormone in the regulation of root development, several of which even hint toward a complex signaling pathway (1, 3, 4, 7).

Supported by the colocalization *thalian* of the signaling components in the nucleus, strigolactone signaling has been suggested to function through the induction of transcriptional changes. However, despite the availability of several transcriptome data sets (30–33), strigolactone-regulated transcription factors and strigolactone-responsive genes are rare, of which *BRANCHED1* (*BRC1*) is one of the best known in *Arabidopsis thaliana* (34). On the whole, only a few differentially expressed genes, often with low differences in expression levels, were identified upon *rac*-GR24 treatment, a synthetic strigolactone analog (31–34). Of last, several studies have emerged that support strigolactone signaling occurring to a large extent at the protein level (29, 35, 36), as illustrated by the direct effect of strigolactones on PIN-FORMED1 (PIN1) recycling at the plasma membrane in xylem parenchyma cells that results in modified auxin flows in the stem and, finally, altered shoot branching (35, 37).

Here we executed a proteome-wide study to gain insight into the intricate strigolactone signaling network in the roots. To this end, we adopted a mass spectrometry-driven, quantitative proteomics approach to compare the profiles of the *max2–1* mutant and wild-type (WT) *Arabidopsis* roots in response to *rac*-GR24. This procedure, in concert with an unbiased metabolite profiling experiment, revealed that MAX2-dependent and *rac*-GR24-induced changes in protein abundance give rise to specific changes in the root metabolome. We used this knowledge to further dissect the link between signaling pathways stimulated by *rac*-GR24 and flavonol accumulation in the root.

EXPERIMENTAL PROCEDURES

Plant Material—Seeds of *Arabidopsis thaliana* (L.) Heynh. (accession Columbia-0) plants were surface sterilized with consecutive treatments of 70% (v/v) ethanol with 0.05% (w/v) sodium dodecyl sulfate (SDS), and then washed with 95% (v/v) ethanol. For material destined to proteomics experiments or RNA preparation, seeds were sown on nylon meshes (20 μm) placed on half-strength Murashige and Skoog (MS) medium containing 1% (w/v) sucrose. Fifty seeds were sown per plate in two rows of 25 and were stratified for 2 days at 4 °C, whereafter the plantlets were grown for 5 days, before being transferred to mock-treated medium or medium containing 1 μM *rac*-GR24. For high-performance thin-layer chromatography (HPTLC) analysis, seeds were stratified for 2 days at 4 °C, whereafter the plantlets were grown for 5 days either on mock or *rac*-GR24-containing medium before methanol extraction. All plants were grown at 21 °C under permanent light conditions.

The *rac*-GR24 that was used for the proteome and the metabolite profiling contained both the $GR24^{5DS}$ (GR24+) and $GR24^{ent-5DS}$ (GR24-) enantiomers (18). In experiments designed to test the effect of the stereochemistry on the flavonol response, purified enantiomers, GR24+ and GR24-, were applied separately.

Time-Resolved Quantitative Proteomics—The roots of 5-day-old *Arabidopsis* WT and *max2–1* plants were transferred to MS medium containing 1% (w/v) sucrose and either 1 μM *rac*-GR24 or 100 μl of the acetone carrier, harvested, and snap-frozen in liquid nitrogen at given time points. Tissues were thawed in 1.5 ml extraction buffer (1% (w/v) CHAPS, 0.5% (w/v) sodium deoxycholate, 0.1% (w/v) SDS, 5 mM EDTA, 10% (v/v) glycerol in phosphate buffered saline, pH 7.5) and a protease inhibitor mixture according to the manufacturer's instructions (Roche Diagnostics, Vilvoorde, Belgium).

Lysates were incubated for 30 min on ice before centrifugation at 16,000 × *g* for 20 min at 4 °C to remove any debris. Samples were desalted over a NAP-10 column (GE-Heathcare, Little Chalfont, UK) with 1 ml of 20 mM triethylammonium bicarbonate buffer. Protein concentrations were measured with the Bradford DC assay (Bio-Rad, Hercules, CA, USA) to keep 400 μg of protein material for the following steps. Samples were digested with endoproteinase-LysC (Sigma-Aldrich, St. Louis, MO) and incubated overnight at 37 °C with gentle agitation.

Because of the reference pool design, samples were divided into two equal parts. One half of each sample was pooled together to produce a reference sample and the other half was maintained to represent the sample itself. The samples were labeled differentially: the reference pool with heavy $^{13}C_3$-propionate and the individual samples with light $^{12}C_3$-propionate as described (38). Labeling was followed by quenching of *N*-hydroxysuccinimide esters with 40 mM glycine to remove excess NHS esters, followed by 80 mM hydroxylamine (NH_2OH) to revert O-propionylation of Ser (S), Thr (T), and Tyr (Y). Individual samples were mixed in a one-to-one ratio with the reference pool (checked on a single shot pre-run on a XL linear trap quadrupole (LTQ) Orbitrap (Thermo Fisher Scientific, Waltham, MA)).

RP-HPLC Fractionation of Peptide Mixtures—Peptides were separated on a 2.1 mm internal diameter (I.D.)×150 mm column (Zorbax®, 300 SB-C18 Narrowbore, Agilent Technologies, Santa Clara, CA) preceded by a C8 pre-column. A 140-min gradient was used with HPLC solvent A, consisting of 10 mM ammonium acetate (pH 5.5) in HPLC grade 98/2 (v/v) water/acetonitrile and solvent B composed of 10 mM ammonium acetate (pH 5.5) in HPLC grade 30/70 (v/v) water/acetonitrile to fractionate in one-minute-wide fractions and finally pooled into 20 fractions for liquid chromatography-tandem mass spectrometry (LC-MS/MS) analysis. Thirty minutes before the samples were injected for reverse-phase (RP)-HPLC, a methionine oxidation step was carried out by adding 3% (v/v) H_2O_2. Tris(2-carboxyethyl)phosphine was added to a final concentration of 2 mM to reduce S-S bridges just before the injection. Samples were vacuum-dried and resuspended in 20 μl of solvent A' (2% (v/v) acetonitrile with 0.1% (v/v) trifluoroacetic acid). The obtained peptide mixtures were introduced into the Ultimate 3000 RSLC nano LC-MS/MS system (Dionex, Sunnyvale, CA) connected in-line to a hybrid LTQ Orbitrap Velos (Thermo Fisher Scientific). The sample mixture was loaded on an in-house-made trapping column (100 μm I.D. × 20 mm, 5-μm C18 Reprosil-HD beads (Dr. Maisch)). After back-flushing from the trap-

ping column, the sample was loaded on an in-house-made analytical reverse-phase column (75 μm I.D. × 150 mm, 5-μm C18 Reprosil-HD beads (Dr. Maisch, Ammerbuch-Entringen, Germany)). Of the peptide mixture, 6 μl was loaded with solvent A' and separated with a linear gradient from 2% (v/v) solvent A" (0.1% (v/v) formic acid) to 50% (v/v) solvent B" (0.1% (v/v) formic acid and 80% (v/v) acetonitrile) at a flow rate of 300 nL/min followed by a wash with 100% solvent B".

LC-MS/MS Analysis and Peptide Identification—The mass spectrometer was operated in data-dependent mode, automatically switching between MS and MS/MS acquisition for the 10 most abundant peaks in a given MS spectrum. In the LTQ-Orbitrap Velos (Thermo Fischer Scientific), full-scan MS spectra were acquired at a target value of 1E6 with a resolution of 60,000. The 10 most intense ions were isolated for fragmentation in the linear ion trap, with a dynamic exclusion of 20 s. Peptides were fragmented after filling the ion trap at a target value of 1E4 ion counts. The MS/MS spectra were searched with the MaxQuant software (version 1.4.0.3) (39, 40) against The Arabidopsis Information Resource (TAIR10_pep_20101214 containing 27,416 protein-coding genes) database, with a precursor mass tolerance set at 10 ppm for the first search (used for nonlinear mass recalibration) and at 4.5 ppm for the main search. Methionine oxidation was searched as fixed modification, whereas variable modifications were set for pyroglutamate formation of amino-terminal glutamine and acetylation of the protein N terminus. Mass tolerance on peptide precursor ions was fixed at 10 ppm and on fragment ions at 0.5 Da. The peptide charge was set to 2+,3+. The instrument was put on electrospray ionization-TRAP. Endoproteinase-LysC was the selected protease, with one missed cleavage allowed; cleavage was accepted as well when lysine was followed by proline. Only peptides were withheld that ranked first and scored above the 99% confidence threshold score. $^{13}C_3$-propionate and $^{12}C_3$-propionate were used as heavy and light labels, respectively, with specificity for lysines and peptide N termini. The feature "matching between runs" was activated. The false discovery rate (FDR) for peptide and protein was set to 1% and the minimum peptide length was set to 7. All mass spectrometry proteomics data have been deposited to the ProteomeXchange Consortium via the PRIDE partner repository with the PRIDE accession PXD003879. The results can be accessed through MS-Viewer (41) on the Protein Prospector website (http://prospector2.ucsf.edu/prospector/cgi-bin/msform.cgi?form=msviewer) with the Search Key: ls5iutdkzh.

Statistical Analysis of the Shotgun Proteomics Data—We first applied a stringent filter to the data set, keeping only protein for which at least two valid values were available from the four biological repeats for every condition tested. The remaining 1,968 proteins were analyzed by fitting a linear mixed model of the following form:

$$Y_{ijkl} = \mu + \beta_i + g_j + m_k + t_l + gm_{jk} + gt_{jl} + mt_{kl} + gmt_{jkl} + \varepsilon_{ijkl} \quad \text{(Eq. 1)}$$

partitioning the variation in protein abundances (Y_{ijkl}) into fixed genotype effects (WT and *max2* represented by g_j), treatment effects (mock and strigolactone represented by m_k), time effects (0 h, 9 h and 24 h for mock, 9 h and 24 h for strigolactone represented by t_l) and all interaction effects, and random block effects, referring to the biological replicates. The genotype.treatment interaction effect is one of the highest importance because it assesses whether the difference in response between the two genotypes is affected by the treatment (averaged over the time series). Random block effects in the model were assumed to be independent and normally distributed with means zero and variance σ^2. The linear mixed model was fitted by the residual maximum likelihood (REML) approach as implemented in Genstat v17 (For details see Payne, R.W. (2013) Genstat Release 17 Reference Manual, Part 3: Procedure library PL24. Oxford: VSN International, Hemel Hempstead, UK). Significance of the fixed main and interaction effects was assessed by an *F*-test.

The distributions of the *p* values for the treatment effect, the genotype effect and the genotype.treatment effect were assessed. Only for the genotype effect we have estimated the FDR to correct for multiple hypotheses testing, considering the large number of proteins significant for this term.

Metabolite Profiling: LC-MS Conditions—For the LC-MS analysis, an Acquity Ultra-Performance Liquid Chromatography (UPLC) system was used connected to a Synapt Q-TOF high-definition MS system (Waters, Milford, MA). Chromatographic separation was done by injecting a 15-μl aliquot on an Acquity BEH C18 column (2.1 mm I.D. × 150 mm, 1.7 μm beads; Waters) with a gradient elution. Mobile phases consisted of water containing 1% (v/v) acetonitrile and 0.1% (v/v) formic acid (A) and acetonitrile containing 1% (v/v) water and 0.1% (v/v) formic acid (B). All solvents used were ULC/MS grade (Biosolve Chemie, Dieuze, France). Water was produced by a DirectQ-UV water purification system (Millipore). The column temperature was maintained at 40 °C and the autosampler temperature at 10 °C. A flow rate of 350 μl/min was applied during the gradient elution starting at time 0 min 5% (B), 30 min 50% (B), and 33 min 100% (B). The eluant was directed to the mass spectrometer equipped with an electrospray ionization source and lock spray interface for accurate mass measurements. MS source parameters were: capillary voltage 2.5 kV, sampling cone 37 V, extraction cone 3.5 V, source temperature 120 °C, desolvation temperature 400 °C, cone gas flow 50 L/h, desolvation gas 550 L/h. The collision energy for trap and transfer cells was set at 4 V and 3 V, respectively. For data acquisition, the dynamic range enhancement mode was activated. Full-scan data were recorded in negative centroid V-mode with a mass range between *m/z* 100–1000 and a scan speed of 0.2 s/scan by means of the Masslynx software (Waters). Leu-enkephalin (400 pg/μl solubilized in water/acetonitrile (1:1, v/v) acidified with 0.1% (v/v) formic acid) was used for the lock mass calibration by scanning every 10 s with a scan time of 0.5 s; three scans were averaged. For MS/MS purposes, the same settings were applied, except that the trap collision energy was ramped from 10 V to 45 V.

For the LC-MS data processing, the Progenesis QI software v 2.0 (Nonlinear Dynamics, Durham, NC) was used to align all chromatograms and to analyze statistically the ArcSinh-transformed compound intensities (normalized to dry weight) through principal component analysis and analysis of variance (*p* value threshold = 0.01). Descriptive statistics were calculated by EZinfo extension (v 3.0) (Umetrics, San José, CA) on Pareto-scaled compound intensities.

RNA Extraction and Quantitative (q)RT-PCR—Roots from WT and *max2–1* plants were harvested and snap-frozen in liquid nitrogen 24 h post treatment (hpt). Cell walls were disrupted by 3-mm metal beads in 2-ml tubes (Eppendorf, Hamburg, Germany) with a mixer mill 400 (Retsch, Haan, Germany) for 2 min at 20 Hz. RNA was extracted and purified with the RNeasy mini kit (Qiagen, Hilden, Germany). Genomic DNA was removed by DNase treatment and the samples were purified by ammonium acetate (2.5 M final concentration) precipitation. Concentrations were measured with a ND-1000 Spectrophotometer (Thermo Fisher Scientific Nanodrop). The iScript cDNA synthesis kit (Bio-Rad) was used to reverse transcribe RNA. qRT-PCR primers were designed with the Quant Prime website software. SYBR Green detection was used during qRT-PCR run on a Light Cycler 480 (Roche Diagnostics). Reactions were done in triplicate in a 384-multiwell plate, in a total volume of 5 μl and cDNA fraction of 10%. Cycle threshold values were obtained and analyzed with the 2-ΔΔCT method (42). The values from four biological repeats and three technical repeats were normalized against those of *ACTIN2* (*ACT2*, AT3G18780) that was used as an internal standard. Normalized val-

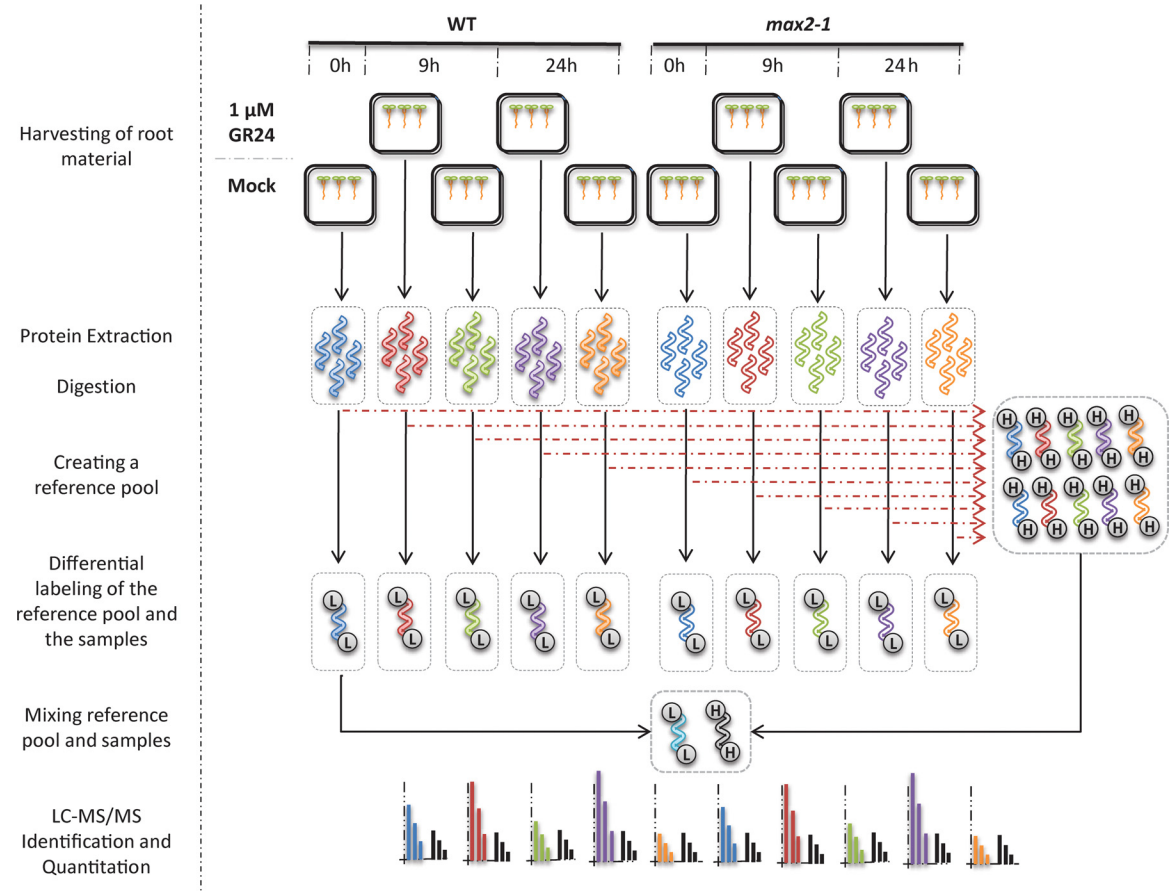

FIG. 1. **Experimental set-up for the protein profiling experiment.** WT and *max2–1* plants were grown for 5 days before transfer to media containing 1 µM *rac*-GR24 (GR24) or the acetone carrier (mock). Root tissue was harvested at 0 h, 9 h, and 24 h post treatment (hpt) for samples treated with only acetone and 9 h and 24 h post treatment for samples treated with GR24. Protein extraction, endoproteinase-LysC digestion, and peptide labeling were done as described (see Experimental Procedures). To produce a reference labeling pool, half of each sample was mixed together. The individual samples were mixed with equal amounts of the reference pool. Samples were fractionated by RP-HPLC and pooled into 20 fractions that were analyzed by LC-MS/MS. Spectra were subsequently searched and analyzed with MaxQuant and Perseus. Quantified proteins were filtered and only those that had valid values for at least three of the four biological repeats of each sample were retained for final analysis.

ues were analyzed according to the published model (43) with the mixed model procedure, Kenilworth, NJ (SAS Institute, Cary, NC).

HPTLC Diphenylboric Acid 2-Amino Ethyl Ester (DPBA) Staining—For the HPLTC analysis of roots, methanol extracts from four biological repeats were prepared from 5-day-old *Arabidopsis* plants grown on 1% (v/v) MS medium containing either 1 µM *rac*-GR24 or 100 µl of the acetone carrier. Roots were harvested. After a methanol extraction, samples were dried with a concentrator 5301 (Eppendorf). The dried samples were resuspended in 20 µl of an 80% (v/v) methanol solution. The concentrated extract was analyzed by HPTLC. Of the mixture, 2 µl was spotted onto a 20 cm × 10 cm silica-60 HPTLC glass plate (Merck) and placed in a glass tank with a Whatman paper wick of 18 cm by 9 cm (Thermo Fisher Scientific) and a mobile polar phase consisting of ethyl acetate, dichloromethane, acetic acid, formic acid, and water in a 100:25:10:10:11 ratio, respectively. After addition of the mobile phase, the glass tank was sealed with silicone grease and gels were run for 25 min. Gels were stained by spraying a methanol solution containing 1% (v/v) DPBA. Plates were placed into an HB-1000 Hybridizer (Thermo Fisher Scientific) at 100 °C for 10 min, whereafter the plates were sprayed with a 5% (v/v) methanol solution containing 4000-polyethylene glycol to stabilize the DPBA compound. Plates were observed after UV excitation at 350 nm. Pictures were taken with a D90 camera (Nikon, Tokyo, Japan).

RESULTS

Proteome Profiling Reveals Differences Between WT and max2–1 Roots upon rac-GR24 Treatment—To gain insight into the *rac*-GR24-induced signaling pathway and the role of MAX2 in the roots, we used *max2–1* and WT *Arabidopsis* (accession Columbia-0) roots to study differences in protein abundance by means of a time-resolved, quantitative proteomics approach. Five-day-old plants were transferred to control (mock) medium or medium containing 1 µM of a *rac*-GR24 mixture for either 9 or 24 h. This experiment was conducted in four biological replicates (Fig. 1).

A reference pool was created by mixing half of each digested proteome extract and labeling the resulting peptide pool with $^{13}C_3$-propionate tags. The peptides of the individual samples were labeled with $^{12}C_3$-propionate. After each indi-

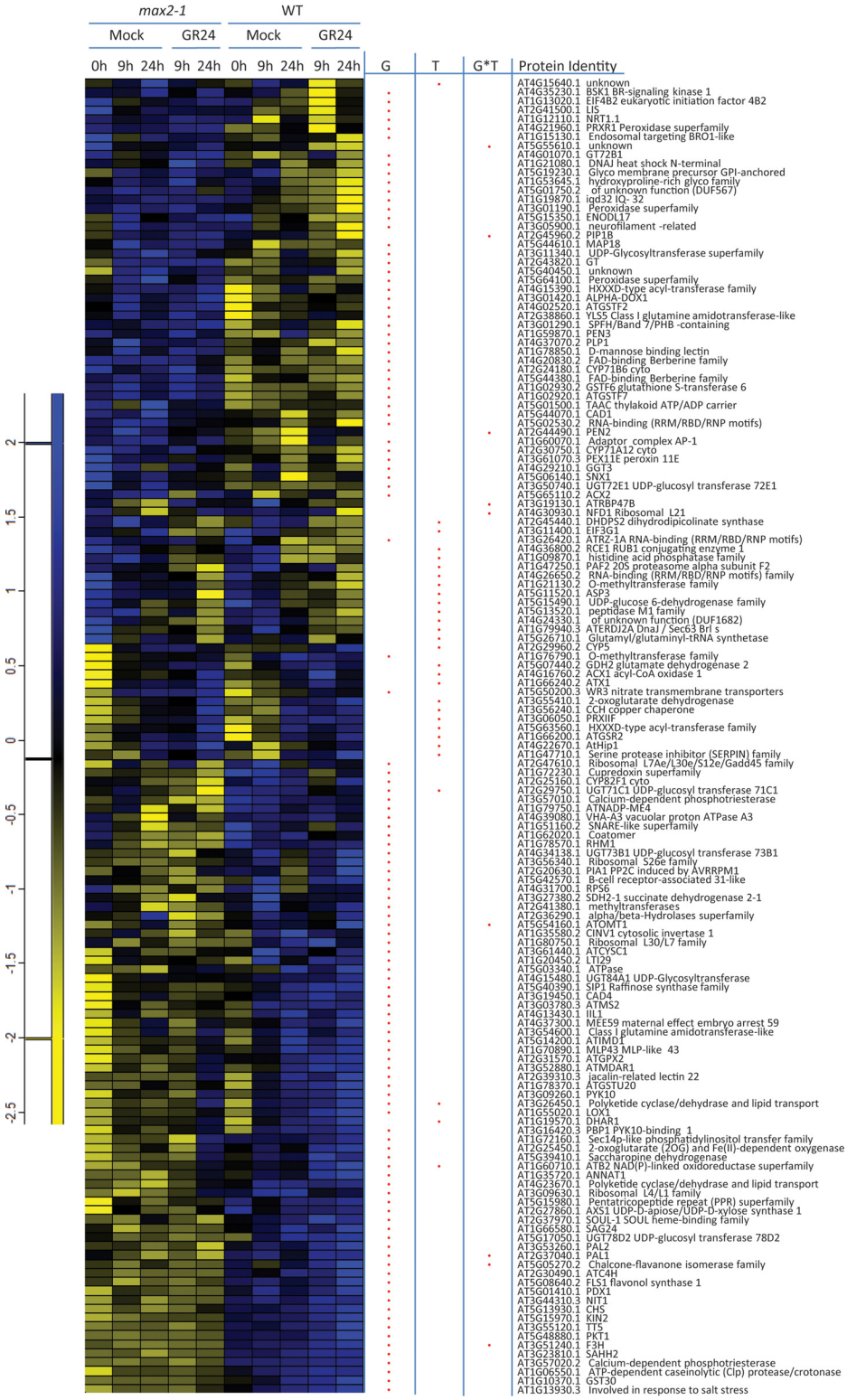

FIG. 2. **Differential molecular responses in *max2–1* and WT roots either mock grown or treated with *rac*-GR24.** Heat map showing average log2 values of protein ratios of four biological repeats (z-scored for graphical representation). Levels are shown for WT and *max2–1* plants grown under mock conditions (0 h, 9 h and 24 h) or after treatment (9 h and 24 h) in the presence of 1 μM *rac*-GR24. The columns labeled G, T, and T*G indicate whether the protein abundance was detected as statistically significantly different between genotypes, treatment, and interaction of both factors, respectively. Only the proteins that are significantly different with a p value <0.01 (red dots) in at least one of the terms are presented.

vidual sample had been mixed with an equal amount of the reference pool, the peptides were prefractionated by RP-HPLC to reduce the sample complexity prior to LC-MS/MS analysis (Fig. 1). This set-up enabled the identification of proteins of which the abundances depended on MAX2, the *rac*-GR24 treatment, or both.

In total, 4,260 proteins were identified and quantified. To increase the stringency of our analysis, we kept only proteins

with valid quantification values in at least two of the four biological replicates for every condition tested. As a result, a subset of 1,968 proteins was retained and subsequently a linear mixed model was fitted to the log-transformed data to assess the genotype {WT and *max2–1*} and treatment {mock, strigolactone} main effects and the genotype.treatment interaction on protein abundance. Fig. 2 shows all proteins for which at least one of the terms (genotype, treatment, or their interaction) was significant with $p < 0.01$ (red dots). All ratio values for these proteins are given in supplemental Table S1. In total, 33 proteins at *p* value <0.01 differed significantly in abundance after *rac*-GR24 treatment, whereas 117 (*p value* <0.01) were differentially abundant when the root proteomes of *max2–1* and WT plants were compared (Fig. 2). Finally, the interaction between treatment and genotype had a statistically significant effect on the abundance of 9 ($p < 0.01$) proteins (Fig. 2). Ratios of all proteins as well as *p* values (when the proteins were included in the statistical analysis), are given in supplemental Table S2.

Upon examination, four out of the nine proteins that have a significant interaction term (genotype.treatment) have been shown to be involved in different steps of flavonoid biosynthesis. For three of these proteins, phenyl ammonia-lyase (PAL1), CFI family protein and flavanone 3′-hydroxylase (F3′H), their abundance increases only in the WT upon *rac*-GR24, suggesting that a functional MAX2 protein is necessary for this change to occur (Fig. 3). More broadly, multiple proteins involved in the flavonoid metabolism are significant for the genotype term, including PAL2, and enzymes more specifically involved in flavonoid biosynthesis and transport, such as flavonol synthase 1 (FLS1), flavanone 3-hydroxylase (F3H), chalcone synthase (CHS), UDP-glucosyl transferase 78D2 (UGT78D2), cinnamate-4-hydroxylase (C4H), and the nonintrinsic ABC protein 9 (NAP9). These proteins were more abundant in WT than in *max2–1* roots. Taken together, these results suggest that in the absence of a functional MAX2, a large set of enzymes responsible for flavonol biosynthesis are less present and that at least for some of these enzymes, their abundance increases in a MAX2-dependent manner upon *rac*-GR24 treatment.

Transcript Analysis Reveals a MAX2-Dependent rac-GR24-Induced Regulation of Genes Coding for Flavonoid Biosynthesis Enzymes—With a detected enrichment for proteins involved in phenylpropanoid and, more specifically, flavonoid synthesis, we wanted to investigate whether these changes between genotype and/or upon *rac*-GR24 treatment were regulated at the transcript level. WT and *max2–1* roots grown in the presence or absence of *rac*-GR24 were used to study the gene expression of markers for phenylpropanoid and flavonol biosynthesis, such as enzymes catalyzing early steps of the phenylpropanoid pathway (*PAL1* and *PAL2*) and proteins more specifically involved in flavonol biosynthesis (*CHS*, *UGT78D2*, and *F'3H*) via qRT-PCR analysis. For all genes tested, no differences in expression levels were detected

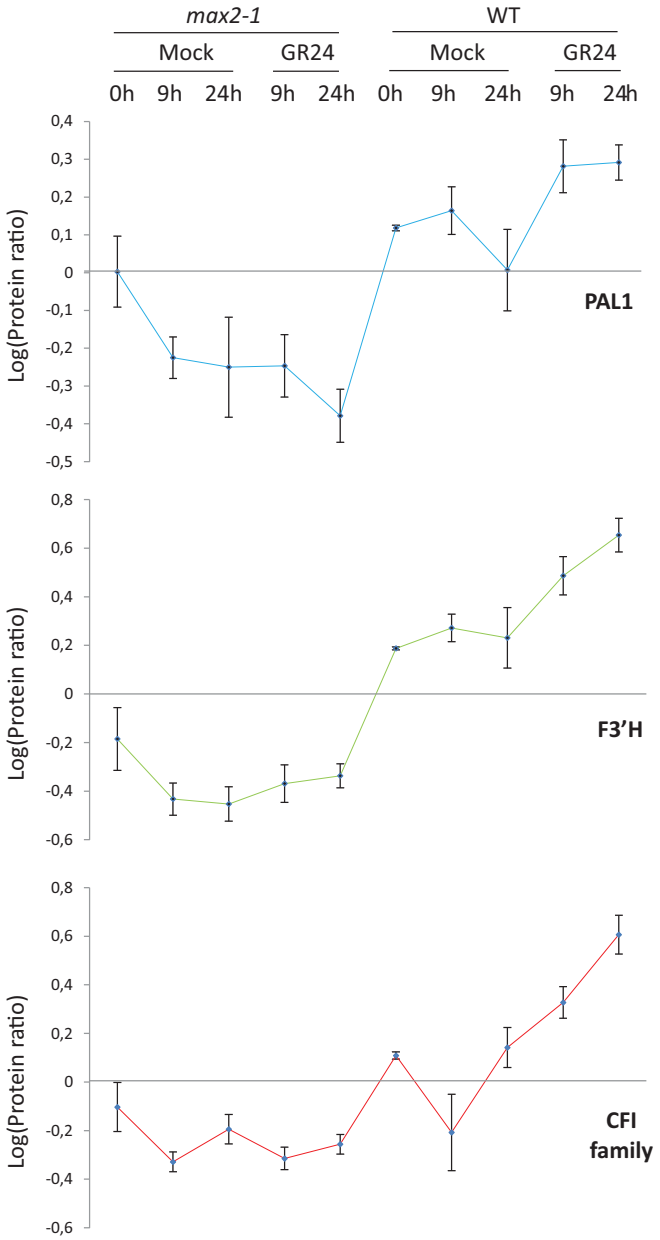

FIG. 3. **Protein abundance profile of flavonol biosynthesis-related proteins.** Protein ratios for flavonol biosynthesis-related proteins (PAL2, CFI family protein, and F3′H) in WT and *max2–1* backgrounds under mock conditions and after *rac*-GR24 treatment.

when untreated WT and *max2–1* samples were compared (Fig. 4). In contrast, the transcript levels of all tested genes increased statistically significantly (Student's *t* test with $p < 0.05$) upon *rac*-GR24 treatment in WT background, a response that was completely abolished in the *max2–1* mutant. These results indicate that the flavonoid biosynthesis pathway is transcriptionally activated by *rac*-GR24 treatment in a MAX2-dependent manner.

Secondary Metabolite Profiling Pinpoints Specific Flavonols to Accumulate upon rac-GR24 Treatment in a MAX2-Depen-

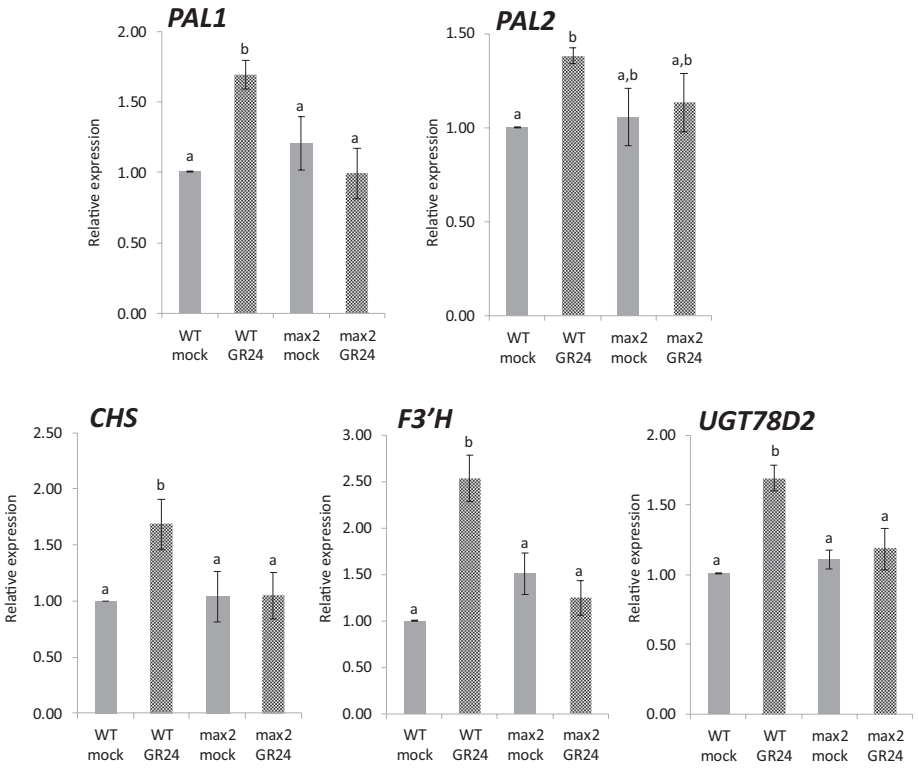

FIG. 4. **MAX2-dependent *rac*-GR24-induced transcriptional regulation of marker genes for phenylpropanoid and flavonol biosynthesis.** Relative transcript levels for two phenylpropanoid biosynthesis genes (*PAL1* and *PAL2*) and three flavonol biosynthesis genes (*CHS, F'3H,* and *UGT78D2*) in WT and *max2–1* backgrounds under mock conditions and after 24 h of *rac*-GR24 treatment.

dent Manner—As *rac*-GR24 treatment and MAX2 function appeared to regulate enzymes involved in flavonoid biosynthesis and, more generally, phenylpropanoid biosynthesis, at the transcript and protein levels, metabolite profiling experiments were conducted. In a first experiment, methanol extracts from the roots of WT plants grown on mock or *rac*-GR24-containing medium were compared and, in a second experiment, metabolite profiles of untreated root tissues of WT and *max2–1* plants were evaluated (Fig. 5*A*). Methanol extracts were analyzed via Ultra-HPLC-MS (for details, see Experimental Procedures).

In total, 1,121 compound ions were detected in experiment 1 (Fig. 5*A*). Prior to univariate analysis, two filters were applied to increase the stringency. An intensity threshold of 500 spectrum counts in at least one group and an average peak width threshold of minimum 0.05 min in at least one group were applied, resulting in 474 remaining compound ions. By Student's *t* test analysis and multiple testing corrections, 93 and 48 compound ions were found to be significantly more and less abundant, respectively, in WT upon *rac*-GR24 treatment (Fig. 5*A*). A principal component analysis (Fig. 5*B*) was carried out and showed a separation between two groups, indicating that plants grown on mock-treated medium or on *rac*-GR24-supplemented medium had different phenolic profiles.

In the second experiment, 1,512 compound ions were detected. With the same filters as in experiment 1, 701 compound ions remained for univariate analysis. The Student's *t* test analysis indicated that 134 and 167 compound ions were significantly more and less abundant, respectively, in *max2–1* mutants. The second principal component analysis (Fig. 5*B*) showed difference in the phenolic profiles of *max2–1* and WT roots grown under mock conditions.

After manual fragment ion clean-up and assessment of numbers and types of compound ions that displayed a MAX2-dependent and *rac*-GR24-induced profile, 28 compounds were retained from the two combined experiments (supplemental Table S3) that could be structurally characterized based on MS/MS fragmentation (Fig. 5*A*). Nine compounds could be classified as phenylpropanoids, such as several glycosyl derivates of *p*-coumaric acid, caffeic acid, and ferulic acid, two as guaiacylglycerol-β-ferulic acid ethers, 11 as flavonols, and one as flavanone naringenin (supplemental Table S3; Fig. 5*A*). Regarding the flavonols, derivates from each of the three main flavonol families, kaempferol, quercetin, and isorhamnetin, accumulated in WT roots upon *rac*-GR24 treatment and were less abundant in *max2–1* mutants than in WT plants (supplemental Table S3). These phenolic profiling results indicate that *rac*-GR24 treatment gives rise to a MAX2-mediated flavonol accumulation in *Arabidopis* roots, in line

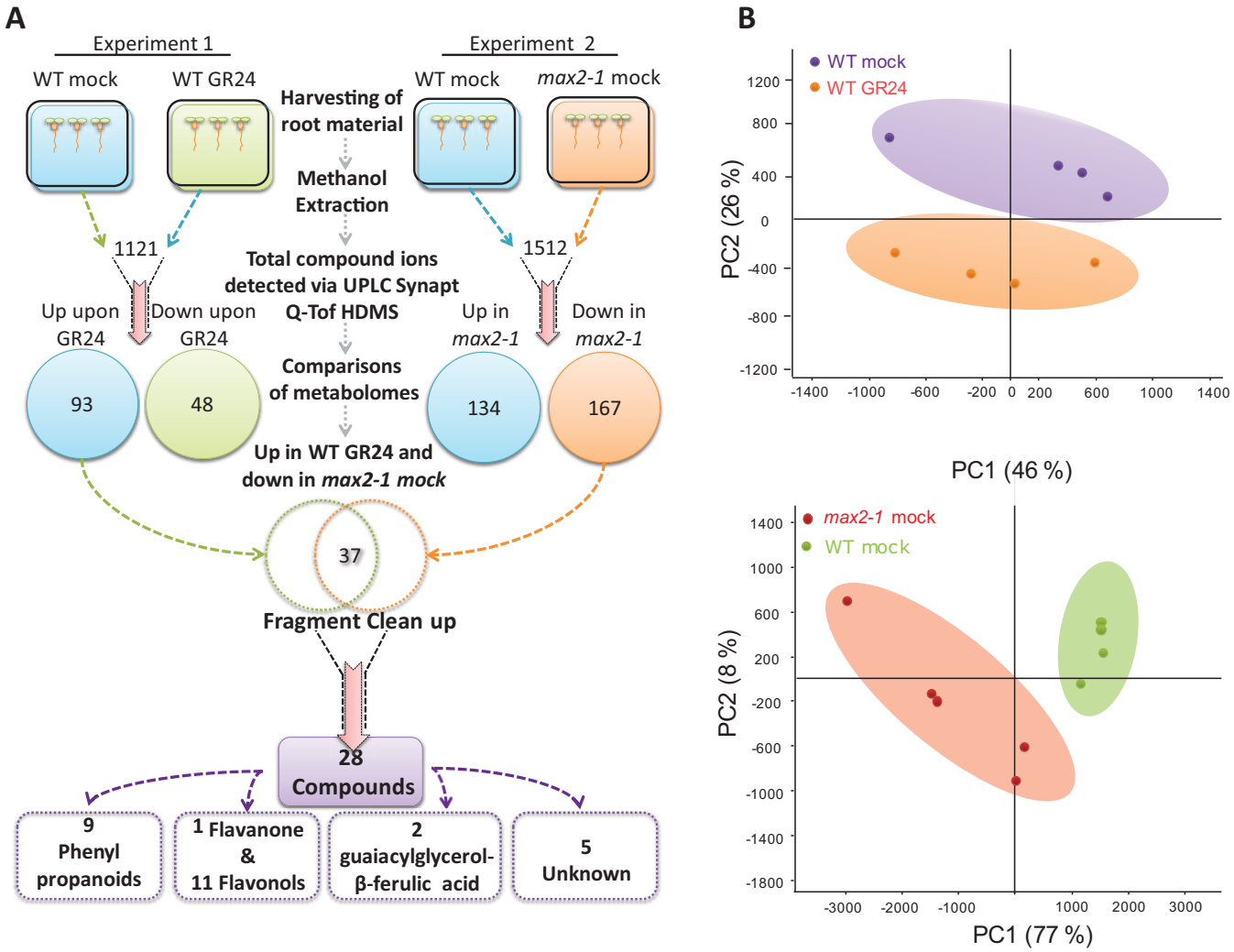

FIG. 5. **Metabolite profiling of *max2–1* and WT roots with and without *rac*-GR24 treatment.** *A,* Outline of the strategy. Two separate metabolomics experiments were done. In the first, WT plants were grown on *rac*-GR24-containing medium or mock medium for 5 days for comparison. In the second experiment, metabolites from WT roots were compared with those from *max2–1* roots after 5 days of growth. In total, 2,633 compounds were identified. After an abundance filter, 37 compounds were found to be upregulated upon *rac*-GR24 treatment and downregulated in *max2–1* compared with WT. Clean-up of fragments reduced this number to 28 compounds, of which five were unknown, nine were lignin precursors, two were guaiacylglycerol-β-ferulic acid ethers, and 12 were flavanones or flavonols. *B,* Principal component analysis plot showing difference when WT and *max2–1* samples and mock and *rac*-GR24-treated samples are compared.

with the abundance profiles of the biosynthesis enzymes and the transcript profiles of the corresponding genes.

A New Flavonol Readout to Dissect Strigolactone Signaling—To confirm the MAX2-dependent *rac*-GR24 metabolic response in roots, we separated methanol extracts on HPTLC, followed by flavonol-specific DPBA staining and UV/VIS spectrophotometry. Firstly, to independently confirm the large-scale metabolome analysis, new methanol extracts were prepared from roots of WT and *max2–1* plants grown with or without *rac*-GR24. *Rac*-GR24 treatment of WT roots resulted in the accumulation of compounds stained mainly orange and blue, corresponding to quercetin and kaempferol derivates, respectively (Fig. 6*A*). Furthermore, this *rac*-GR24-triggered flavonol accumulation was abolished in the *max2–1* mutant background (Fig. 6*A*), confirming the UHPLC-MS data that revealed an increase in flavonol production upon *rac*-GR24 treatment in roots.

The applied *rac*-GR24 consisted of two enantiomers, $GR24^{5DS}$ (GR24+) and $GR24^{ent\text{-}5DS}$ (GR24-), thought to mimic naturally occurring strigolactones and potentially karrikins or other unknown compounds, respectively (18). Next, the specificity of the observed flavonoid response to one of the two enantiomers was evaluated. Flavonols accumulated after treatment with both 1 μM GR24+ or 1 μM GR24- in roots of 5-day-old plants (Fig. 6*B*). Additionally, the roles were examined of the two receptor proteins D14 and HTL/KAI2 that can mediate the response to *rac*-GR24 (17) in the observed strigolactone response. The *d14* mutant still accumulated

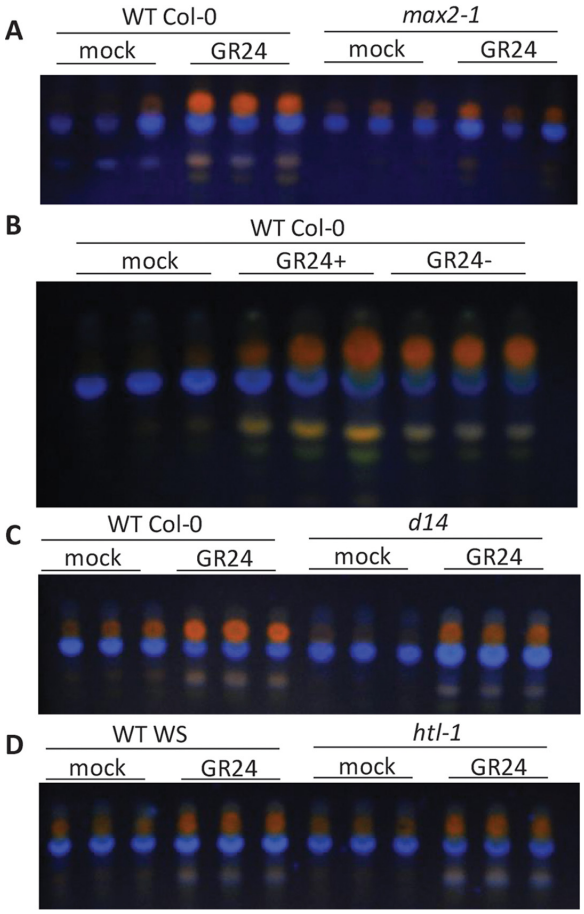

FIG. 6. **Visualization of flavonol induction on HPTLC plates.** *A,* HPTLC plate with DPBA-stained methanol extracts from WT and *max2–1* roots treated with *rac*-GR24 or not. *B,* HPTLC plate with DPBA-stained methanol extracts from a mock-treated WT root and grown either with 1 μM GR24+ or 1 μM GR24-. *C,* HPTLC plate with DPBA-stained methanol extracts from a mock-treated WT root and *d14* mutant roots grown either with 1 μM GR24+ or 1 μM GR24-. *D* HPTLC plate with DPBA-stained methanol extracts from a mock-treated WT (accession Wassilewskija (WS)) root and a *htl-1* mutant root grown either with 1 μM GR24+ or 1 μM GR24-.

flavonols in response to *rac*-GR24 (Fig. 6*C*) as did the *htl-1*/*kai2* mutant, available in the *Arabidopsis* Wassilewskija (Ws) accession and responding similarly as the Ws control (Fig. 6*D*). Taken together, these results show that the uncovered flavonol response is common to both *rac*-GR24-containing enantiomers and can be induced both through D14 and/or KAI2.

DISCUSSION

With the present study, we shed more light on the processes that are at play downstream of the *rac*-GR24 perception and underline the multiplicity of roles played by MAX2 in the roots of *Arabidopsis*. A protein profiling approach led to the identification of 4,260 proteins in the root proteome in four biological replicates. By means of a linear mixed model analysis of variance, a total of 147 proteins displayed a statistically significant difference in abundance (p value < 0.01), either when *max2–1* and WT root proteomes were compared, upon *rac*-GR24 treatment, or because of the interaction of both genotype and treatment.

Interestingly, our data set of significantly regulated proteins presented a clear enrichment for phenylpropanoid/flavonoid metabolism-related proteins, which we further explored via transcriptional and metabolome analyses. For several of the genes encoding these enzymes, qRT-PCR data revealed a MAX2-dependent increase in transcript levels upon *rac*-GR24 treatment. Accordingly, metabolome analysis confirmed the *rac*-GR24-induced accumulation of flavonols requiring a functional MAX2. As flavonol compounds are known to be stress responsive in some cases (44), it is imperative to underline the MAX2-dependent character of this response, hinting at a specific response to *rac*-GR24 and ruling out the possibility that merely a general stress response is observed. On the metabolite level, 11 flavonols, one direct flavonol precursor, naringenin and, more generally, nine phenylpropanoids displayed a MAX2-dependent increase in response to the *rac*-GR24 treatment, supporting a clear link between strigolactones and flavonols in the root. Previously, a *rac*-GR24-triggered induction of *CHS* expression, comparable to the one described here, had been observed in whole seedlings (45), implying that flavonol might accumulate in different plant tissues. Accordingly, a transcriptome analysis has revealed that flavonol biosynthesis genes are induced at lower levels in *max2–1* than in WT upon drought stress in leaves (31). Moreover, flavonol production has been shown to be misregulated in the strigolactone biosynthesis mutant *max1* in the shoot (46). However, because mutants affected in flavonol biosynthesis have no enhanced branching phenotype, flavonols probably do not play a main role in strigolactone-controlled shoot branching (47). As flavonol accumulation and aspects of the root architecture have been linked (48–50), the next challenge will be to examine the role of flavonols in *rac*-GR24-affected processes in the root.

We have translated the connection between strigolactones and flavonols in the root into a cost-effective and user-friendly HPTLC tool that allowed us to acquire more insight into the *rac*-GR24 signaling pathways. Recently, the use of *rac*-GR24 as a generic strigolactone analog has been questioned, because *rac*-GR24 is actually a mixture of two enantiomers. Whereas GR24+ mimics natural strigolactones and is perceived via D14, GR24- is active via the KAI2 receptor and represents a noncanonical strigolactone analog. Importantly, both enantiomers have been shown to signal via MAX2. In this context, some strigolactone-related phenotypes have been linked to specific stereo-isoforms of *rac*-GR24 or specific receptors, although these observations were not absolute (18). On the one hand, shoot branching is elicited by GR24+ via D14 signaling, whereas on the other hand, GR24- and KAI2 affect hypocotyl elongation and aberrant cotyledon morphology (18, 25). Therefore, we tested whether the flavonol

response was specific to an enantiomer receptor pair. The application of the specific enantiomers revealed that both GR24+ and GR24- could increase the flavonol production. In addition, both the *d14* and *kai2* signaling mutants were examined for their capacity to transduce the *rac*-GR24 and give rise to the flavonol read out. In agreement with the enantiomer experiment, the flavonol induction was maintained in both mutants. Together, these results imply that the *rac*-GR24-induced and MAX2-controlled flavonol production is not stereo-selective and, hence, can occur upon activation of either D14 or KAI2. This observation suggests that, at least in the roots, a crosstalk exists between D14 and KAI2 pathways and raises the question whether other known root phenotypes can also be instigated by both receptors.

Besides flavonols, our data indicate that also other secondary metabolites could contribute to strigolactone-mediated effects in *Arabidopsis* roots. Several antioxidant phenylpropanoids, sharing *p*-coumaric acid as a precursor, accumulate with the same strigolactone-related abundance profiles as flavonols. From the proteomics results, we can infer that this effect might be caused by a change in production of CINNAMATE 4-HYDROXYLASE (C4H), the enzyme producing *p*-coumaric acid from cinnamic acid. Moreover, two hexosylated G(8-O-4)ferulic acid compounds were found to accumulate similarly as the flavonols. The *in planta* function of these neolignan-like compounds is unknown, but we can postulate that their accumulation is the consequence of an increase in (hexosylated) ferulic acid.

Previously, a comparable proteome analysis in the context of strigolactone signaling had been conducted (36). Only a limited overlap could be observed with our data (10% at the protein level), potentially arising from technical differences. We used a 5-fold lower concentration of *rac*-GR24 and sampled roots in contrast to whole plants. Nevertheless, a more attractive explanation is also plausible: we used the signaling mutant *max2–1* instead of the biosynthesis mutant *max3*. Thus, the previous approach focused on proteome changes upon signaling of natural strigolactones (36), whereas our work spans an enlarged signaling network, uncovering all downstream effects of MAX2. In this context, it is important to note that the role of MAX2 is broader than strigolactone signaling alone and also to encompass signal transduction of unknown molecules (18, 51). Although not yet biochemically characterized, additional MAX2 activity elicitors are expected to exist based on genetic studies, as illustrated by the increase in LRD in the *max2–1* mutant, which is not phenocopied in the *max3* and *max4* mutants, despite their inability to synthesize strigolactones (1, 2).

Additionally, we detected a set of proteins that responded to *rac*-GR24, both in the *max2–1* background and in the WT control, possibly pointing toward the existence of a MAX2-independent response to strigolactones. In agreement, MAX2-independent responses in root growth and development to *rac*-GR24 were reported (2, 35).

In conclusion, the large set of proteins shown to be regulated by the MAX2 function provides a comprehensive resource that can serve as a foundation for studies aiming to elucidate the roles of MAX2 in roots. Finally, the link between strigolactones and flavonols will allow the dissection of the molecular networks that act between strigolactone signaling and the induction of transcriptional changes.

Acknowledgments—We thank our colleagues Ive De Smet, Sven Degroeve, and Sven Eyckerman for fruitful discussions and Martine De Cock for help in preparing the manuscript.

* This work was supported by Ghent University Hercules program for the UPLC-Synapt Q-Tof HDMS system (grant no. AUGE/014) and European Cooperation on Science and Technology (COST action FA1206). A.W. is the recipient of a VIB International PhD program fellowship. E.S. and R.V. are Postdoctoral Fellows of the Research Foundation-Flanders.

S This article contains supplemental material.

[b] To whom correspondence should be addressed: Department of Plant Systems Biology-Department of Plant Biotechnology and Bioinformatics, VIB-Ghent University, Technologiepark 927, 9051 Gent, Belgium. Tel.: +32 9 3313910; Fax: +32 9 3313809; E-mail: sofie.goormachtig@psb.vib-ugent.be.

[c] These authors contributed equally to this work.

REFERENCES

1. Kapulnik, Y., Delaux, P.-M., Resnick, N., Mayzlish-Gati, E., Wininger, S., Bhattacharya, C., Séjalon-Delmas, N., Combier, J.-P., Bécard, G., Belausov, E., Beeckman, T., Dor, E., Hershenhorn, J., and Koltai, H. (2011) Strigolactones affect lateral root formation and root-hair elongation in *Arabidopsis*. *Planta* **233,** 209–216
2. Ruyter-Spira, C., Kohlen, W., Charnikhova, T., van Zeijl, A., van Bezouwen, L., de Ruijter, N., Cardoso, C., Lopez-Raez, J. A., Matusova, R., Bours, R., Verstappen, F., and Bouwmeester, H. (2011) Physiological effects of the synthetic strigolactone analog GR24 on root system architecture in Arabidopsis: another belowground role for strigolactones? *Plant Physiol.* **155,** 721–734
3. Mayzlish-Gati, E., De-Cuyper, C., Goormachtig, S., Beeckman, T., Vuylsteke, M., Brewer, P. B., Beveridge, C. A., Yermiyahu, U., Kaplan, Y., Enzer, Y., Wininger, S., Resnick, N., Cohen, M., Kapulnik, Y., and Koltai, H. (2012) Strigolactones are involved in root response to low phosphate conditions in Arabidopsis. *Plant Physiol.* **160,** 1329–1341
4. Sun, H., Tao, J., Liu, S., Huang, S., Chen, S., Xie, X., Yoneyama, K., Zhang, Y., and Xu, G. (2014) Strigolactones are involved in phosphate- and nitrate-deficiency-induced root development and auxin transport in rice. *J. Exp. Bot.* **65,** 6735–6746
5. Koltai, H. (2011) Strigolactones are regulators of root development. *New Phytol.* **190,** 545–549
6. Rasmussen, A., Mason, M. G., De Cuyper, C., Brewer, P. B., Herold, S., Agusti, J., Geelen, D., Greb, T., Goormachtig, S., Beeckman, T., and Beveridge, C. A. (2012) Strigolactones suppress adventitious rooting in Arabidopsis and pea. *Plant Physiol.* **158,** 1976–1987
7. Kapulnik, Y., Resnick, N., Mayzlish-Gati, E., Kaplan, Y., Wininger, S., Hershenhorn, J., and Koltai, H. (2011) Strigolactones interact with ethylene and auxin in regulating root-hair elongation in *Arabidopsis*. *J. Exp. Bot.* **62,** 2915–2924
8. Kretzschmar, T., Kohlen, W., Sasse, J., Borghi, L., Schlegel, M., Bachelier, J. B., Reinhardt, D., Bours, R., Bouwmeester, H. J., and Martinoia, E. (2012) A petunia ABC protein controls strigolactone-dependent symbiotic signalling and branching. *Nature* **483,** 341–344
9. Waldie, T., McCulloch, H., and Leyser, O. (2014) Strigolactones and the control of plant development: lessons from shoot branching. *Plant J.* **79,** 607–622
10. Booker, J., Sieberer, T., Wright, W., Williamson, L., Willett, B., Stirnberg, P., Turnbull, C., Srinivasan, M., Goddard, P., and Leyser, O. (2005) *MAX1* encodes a cytochrome P450 family member that acts downstream of

MAX3/4 to produce a carotenoid-derived branch-inhibiting hormone. *Dev. Cell* **8,** 443–449
11. Kohlen, W., Charnikhova, T., Liu, Q., Bours, R., Domagalska, M. A., Beguerie, S., Verstappen, F., Leyser, O., Bouwmeester, H., and Ruyter-Spira, C. (2011) Strigolactones are transported through the xylem and play a key role in shoot architectural response to phosphate deficiency in nonarbuscular mycorrhizal host Arabidopsis. *Plant Physiol.* **155,** 974–987
12. Alder, A., Jamil, M., Marzorati, M., Bruno, M., Vermathen, M., Bigler, P., Ghisla, S., Bouwmeester, H., Beyer, P., and Al-Babili, S. (2012) The path from β-carotene to carlactone, a strigolactone-like plant hormone. *Science* **335,** 1348–1351
13. Abe, S., Sado, A., Tanaka, K., Kisugi, T., Asami, K., Ota, S., Kim, H. I., Yoneyama, K., Xie, X., Ohnishi, T., Seto, Y., Yamaguchi, S., Akiyama, K., Yoneyama, K., and Nomura, T. (2014) Carlactone is converted to carlactonoic acid by MAX1 in *Arabidopsis* and its methyl ester can directly interact with AtD14 in vitro. *Proc. Natl. Acad. Sci. U.S.A.* **111,** 18084–18089
14. Sasse, J., Simon, S., Gübeli, C., Liu, G.-W., Cheng, X., Friml, J., Bouwmeester, H., Martinoia, E., and Borghi, L. (2015) Asymmetric localizations of the ABC transporter PaPDR1 trace paths of directional strigolactone transport. *Curr. Biol.* **25,** 647–655
15. Hamiaux, C., Drummond, R. S. M., Janssen, B. J., Ledger, S. E., Cooney, J. M., Newcomb, R. D., and Snowden, K. C. (2012) DAD2 is an α/β hydrolase likely to be involved in the perception of the plant branching hormone, strigolactone. *Curr. Biol.* **22,** 2032–2036
16. Guo, Y., Zheng, Z., La Clair, J. J., Chory, J., and Noel, J. P. (2013) Smoke-derived karrikin perception by the α/β-hydrolase KAI2 from *Arabidopsis. Proc. Natl. Acad. Sci. U.S.A.* **110,** 8284–8289
17. Nelson, D. C., Scaffidi, A., Dun, E. A., Waters, M. T., Flematti, G. R., Dixon, K. W., Beveridge, C. A., Ghisalberti, E. L., and Smith, S. M. (2011) F-box protein MAX2 has dual roles in karrikin and strigolactone signaling in *Arabidopsis thaliana. Proc. Natl. Acad. Sci. U.S.A.* **108,** 8897–8902
18. Scaffidi, A., Waters, M. T., Sun, Y. K., Skelton, B. W., Dixon, K. W., Ghisalberti, E. L., Flematti, G. R., and Smith, S. M. (2014) Strigolactone hormones and their stereoisomers signal through two related receptor proteins to induce different physiological responses in Arabidopsis. *Plant Physiol.* **165,** 1221–1232
19. Stirnberg, P., van de Sande, K., and Leyser, H. M. O. (2002) *MAX1* and *MAX2* control shoot lateral branching in *Arabidopsis. Development* **129,** 1131–1141
20. Stirnberg, P., Furner, I. J., and Leyser, H. M. O. (2007) MAX2 participates in an SCF complex which acts locally at the node to suppress shoot branching. *Plant J.* **50,** 80–94
21. Jiang, L., Liu, X., Xiong, G., Liu, H., Chen, F., Wang, L., Meng, X., Liu, G., Yu, H., Yuan, Y., Yi, W., Zhao, L., Ma, H., He, Y., Wu, Z., Melcher, K., Qian, Q., Xu, H. E., Wang, Y., and Li, J. (2013) DWARF 53 acts as a repressor of strigolactone signalling in rice. *Nature* **504,** 401–405
22. Zhou, F., Lin, Q., Zhu, L., Ren, Y., Zhou, K., Shabek, N., Wu, F., Mao, H., Dong, W., Gan, L., Ma, W., Gao, H., Chen, J., Yang, C., Wang, D., Tan, J., Zhang, X., Guo, X., Wang, J., Jiang, L., Liu, X., Chen, W., Chu, J., Yan, C., Ueno, K., Ito, S., Asami, T., Cheng, Z., Wang, J., Lei, C., Zhai, H., Wu, C., Wang, H., Zheng, N., and Wan, J. (2013) D14–SCFD3 dependent degradation of D53 regulates strigolactone signalling. *Nature* **504,** 406–410
23. Stanga, J. P., Smith, S. M., Briggs, W. R., and Nelson, D. C. (2013) *SUPPRESSOR OF MORE AXILLARY GROWTH2 1* controls seed germination and seedling development in Arabidopsis. *Plant Physiol.* **163,** 318–330
24. Wang., L., Wang, B., Jiang, L., Liu, X., Li, X., Lu, Z., Meng, X., Wang, Y., Smith, S. M., and Li, J. (2015) Strigolactone signaling in Arabidopsis regulates shoot development by targeting D53-like SMXL repressor proteins for ubiquitination and degradation. *Plant Cell* **27,** 3128–3142
25. Soundappan, I., Bennett, T., Morffy, N., Liang, Y., Stanga, J. P., Abbas, A., Leyser, O., and Nelson, D. C. (2015) SMAX1-LIKE/D53 family members enable distinct MAX2-dependent responses to strigolactones and karrikins in Arabidopsis. *Plant Cell* **27,** 3143–3159
26. Sorefan, K., Booker, J., Haurogné, K., Goussot, M., Bainbridge, K., Foo, E., Chatfield, S., Ward, S., Beveridge, C., Rameau, C., and Leyser, O. (2003) *MAX4* and *RMS1* are orthologous dioxygenase-like genes that regulate shoot branching in *Arabidopsis* and pea. *Genes Dev.* **17,** 1469–1474
27. Booker, J., Auldridge, M., Wills, S., McCarty, D., Klee, H., and Leyser, O. (2004) MAX3/CCD7 is a carotenoid cleavage dioxygenase required for the synthesis of a novel plant signaling molecule. *Curr. Biol.* **14,** 1232–1238
28. Bennett, T., and Leyser, O. (2014) Strigolactone signalling: standing on the shoulders of DWARFs. *Curr. Opin. Plant Biol.* **22,** 7–13
29. Pandya-Kumar, N., Shema, R., Kumar, M., Mayzlish-Gati, E., Levy, D., Zemach, H., Belausov, E., Wininger, S., Abu-Abied, M., Kapulnik, Y., and Koltai, H. (2014) Strigolactone analog GR24 triggers changes in PIN2 polarity, vesicle trafficking and actin filament architecture. *New Phytol.* **202,** 1184–1196
30. Mashiguchi, K., Sasaki, E., Shimada, Y., Nagae, M., Ueno, K., Nakano, T., Yoneyama, K., Suzuki, Y., and Asami, T. (2009) Feedback-regulation of strigolactone biosynthetic genes and strigolactone-regulated genes in Arabidopsis. *Biosci. Biotechnol. Biochem.* **73,** 2460–2465
31. Van Ha, C., Leyva-González, M. A., Osakabe, Y., Tran, U. T., Nishimaya, R., Watanabe, Y., Tanaka, M., Seki, M., Yamaguchi, S., Dong, N. V., Yamaguchi-Shinozaki, K., Shinozaki, K., Herrera-Estrella, L., and Tran, L.-S. P. (2014) Positive regulatory role of strigolactone in plant responses to drought and salt stress. *Proc. Natl. Acad. Sci. U.S.A.* **111,** 851–856
32. López-Ráez, J. A., and Bouwmeester, H. (2008) Fine-tuning regulation of strigolactone biosynthesis under phosphate starvation. *Plant Signal. Behav.* **3,** 963–965
33. Mayzlish-Gati, E., LekKala, S. P., Resnick, N., Wininger, S., Bhattacharya, C., Lemcoff, J. H., Kapulnik, Y., and Koltai, H. (2010) Strigolactones are positive regulators of light-harvesting genes in tomato. *J. Exp. Bot.* **61,** 3129–3136
34. Braun, N., de Saint Germain, A., Pillot, J.-P., Boutet-Mercey, S., Dalmais, M., Antoniadi, I., Li, X., Maia-Grondard, A., Le Signor, C., Bouteiller, N., Luo, D., Bendahmane, A., Turnbull, C., and Rameau, C. (2012) The pea TCP transcription factor PsBRC1 acts downstream of strigolactones to control shoot branching. *Plant Physiol.* **158,** 225–238
35. Shinohara, N., Taylor, C., and Leyser, O. (2013) Strigolactone can promote or inhibit shoot branching by triggering rapid depletion of the auxin efflux protein PIN1 from the plasma membrane. *PLoS Biol.* **11,** e1001474
36. Li, Z., Czarnecki, O., Chourey, K., Yang, J., Tuskan, G. A., Hurst, G. B., Pan, C., and Chen, J.-G. (2014) Strigolactone-regulated proteins revealed by iTRAQ-based quantitative proteomics in *Arabidopsis. J. Proteome Res.* **13,** 1359–1372
37. Crawford, S., Shinohara, N., Sieberer, T., Williamson, L., George, G., Hepworth, J., Müller, D., Domagalska, M. A., and Leyser, O. (2010) Strigolactones enhance competition between shoot branches by dampening auxin transport. *Development* **137,** 2905–2913
38. Ghesquière, B., Jonckheere, V., Colaert, N., Van Durme, J., Timmerman, E., Goethals, M., Schymkowitz, J., Rousseau, F., Vandekerckhove, J., and Gevaert, K. (2011) Redox proteomics of protein-bound methionine oxidation. *Mol. Cell. Proteomics* **10,** M110.006866
39. Cox, J., and Mann, M. (2008) MaxQuant enables high peptide identification rates, individualized p.p.b.-range mass accuracies and proteome-wide protein quantification. *Nat. Biotechnol.* **26,** 1367–1372
40. Cox, J., Neuhauser, N., Michalski, A., Scheltema, R. A., Olsen, J. V., and Mann, M. (2011) Andromeda: a peptide search engine integrated into the MaxQuant environment. *J. Proteome Res.* **10,** 1794–1805
41. Baker, P. R., and Chalkley, R. J. (2014) MS-viewer: a web-based spectral viewer for proteomics results. *Mol. Cell. Proteomics* **5,** 1392–1396
42. Livak, K. J., and Schmittgen, T. D. (2001) Analysis of relative gene expression data using real-time quantitative PCR and the $2^{-\Delta\Delta CT}$ method. *Methods* **25,** 402–408
43. Rasmussen, A., Heugebaert, T., Matthys, C., Van Deun, R., Boyer, F.-D., Goormachtig, S., Stevens, C., and Geelen, D. (2013) A fluorescent alternative to the synthetic strigolactone GR24. *Mol. Plant* **6,** 100–112
44. Pollastri, S., and Tattini, M. (2011) Flavonols: old compounds for old roles. *Ann. Bot.* **108,** 1225–1233
45. Waters, M. T., and Smith, S. M. (2013) KAI2- and MAX2-mediated responses to karrikins and strigolactones are largely independent of HY5 in *Arabidopsis* seedlings. *Mol. Plant* **6,** 63–75
46. Lazar, G., and Goodman, H. M. (2006) *MAX1*, a regulator of the flavonoid pathway, controls vegetative axillary bud outgrowth in *Arabidopsis. Proc. Natl. Acad. Sci. U.S.A.* **103,** 472–476
47. Bennett, T., Sieberer, T., Willett, B., Booker, J., Luschnig, C., and Leyser, O. (2006) The *Arabidopsis MAX* pathway controls shoot branching by reg-

ulating auxin transport. *Curr. Biol.* **16,** 553–563
48. Maloney, G. S., DiNapoli, K. T., and Muday, G. K. (2014) The *anthocyanin reduced* tomato mutant demonstrates the role of flavonols in tomato lateral root and root hair development. *Plant Physiol.* **166,** 614–631
49. Nguyen, H. N., Kim, J. H., Hyun, W. Y., Nguyen, N. T., Hong, S.-W., and Lee, H. (2013) TTG1-mediated flavonols biosynthesis alleviates root growth inhibition in response to ABA. *Plant Cell Rep.* **32,** 503–514
50. Santelia, D., Henrichs, S., Vincenzetti, V., Sauer, M., Bigler, L., Klein, M., Bailly, A., Lee, Y., Friml, J., Geisler, M., and Martinoia, E. (2008) Flavonoids redirect PIN-mediated polar auxin fluxes during root gravitropic responses. *J. Biol. Chem.* **283,** 31218–31226
51. Conn, C. E., and Nelson, D. C. (2015) Evidence that KARRIKIN-INSENSITIVE2 (KAI2) receptors may perceive an unknown signal that is not karrikin or strigolactone. *Front. Plant Sci.* **6,** 1219